Static Characteristics of n+-n-p-p+ Silicon IMPATT Diode

Dr. Muneer Aboud Hashem

Electrical Engineering Department ,College of Engineering

Al-Mustansiriya University, Baghdad, Iraq

Abstract

To optimize device performance, theoretical analysis for static characteristics of an n^+-n-p-p^+ silicon IMPATT diode with a deep junction from the surface and a diffused junction in the n-p layer is presented. The doping profile in the (n) layer is considered to be a Chebyshev orthogonal polynomial form, the diffusion coefficient is concentration dependent, and the junction depth varies according to the diffusion time. The most important characteristics such as the electric field distribution, potential distribution, and excess noise factor are treated numerically using Newton's method and the introduction of MATLAB version 6.1. Furthermore, response speed and the figure of merit, the cw output power, are treated. It is found that the electric field and the potential are both increased with increasing junction depth because of the increase in both the depletion layer width and the impurity gradient. The excess noise factor is enhanced with deeper junction since the maximum field is in its highest value. The response speed and the output power are decreasing with wider depletion width and can be enhanced using moderate junction depth.

الخـــلاصـــــة

يعرض البحث التحليل النظري للخواص الساكنة للثنائي السيلكوني الذي يعتمد اسلوب تأين الاصطدام و زمن انتقال حاملات التيار (IMPATT) والمتكون من التركيب (p+-n-p-p+) للوصول الى الاداء الامثل لعمل الثنائي .

الثنائي ممثل بملتقى انتشار بين طبقتي (n) و (p) عميق عن السطح. ان شكل الاشابة في طبقة (n) ممثل بشكل دالةمتعددة الحدود متعامدة ،كما ان معامل الانتشار يعتمد على تركيز طبقة (n) وعمق الملتقى يتغير تبعا لزمن الانتشار.

ان اهم الخواص لهذا الثنائي كتوزيع المجال الكهربائي وتوزيع الجهد ومعامل الضوضاء الزائدة قد تم معالجتها باعتماد اسلوب التحليل العددي باستخدام طريقة Newton وتقديم ال MATLAB النسخة 6.1 لمعالجة العلاقات الرياضية. والابعد من ذلك، تم تحليل كل من سرعة الاستجابة ومعامل الجودة الذي هو قدرة الاشارة المستمرة الخارجة. وقد لوحظ ان المجال الكهربائي والجهد تتناسبان طردياً مع عمق المفرق بسبب الزيادة في كل من عرض منطقة الاستنزاف وازدياد هبوط تركيز الشوائب. كذلك يمكن تحسين معامل الضوضاء الزائدة باستخدام مفرق عميق بسبب وصول المجال الكهربائي الى اعلى قيمة له. ان سرعة الاستجابة و القدرة الخارجة تقل باستخدام مفرق عريض و لكن يمكن تحسينها باستخدام عمق مفرق معتدل.

1. Introduction

Two important characteristics stand for IMPATT diode, impact ionization and transit time to produce negative resistance at microwave frequencies. The device is operated at high reverse-bias voltage for certain avalanche multiplication takes place, the carriers hence drift at a saturation velocity and gain sufficient high energy from the electric field to release new electron-hole pairs through impact ionization. A chain of these impact ionizations leads to carrier multiplication. There is a great difference between impact-ionization coefficients of electrons and holes in silicon. The transit time involved in the IMPATT diode is the depletion layer transit time and the time required for the avalanche to develop, i.e. the avalanche build up time. The IMPATT diode is now one of the most powerful solid-state sources of microwave power [1].The IMPATT diode can generate highest continuous wave power output at millimeter-wave frequencies (i.e., above 30GHZ) of all solid-state devices [2]. The power output is not only the criterion for selecting a device for a certain microwave application, many factors should be taken into consideration. One of these factors is the ease and precise fabrication of the device to eliminate or to reduce parasitic resistances and capacitances. The second factor is the noise that results from the spontaneous fluctuations from the current passing through the device or of voltage developed across the device [3] .

2. Device Model

An n^+-n-p-p^+ silicon IMPATT diode with a deep junction from the surface is the device model depicted in Fig(1), the (n) layer which is the key layer, is made of arsenic diffusion in silicon. The distribution of impurities at any time during the diffusion can be calculated from the solution of diffusion equation with appropriate boundary conditions. The dependence of diffusivity on temperature, as we shall see, explains that high temperatures are required for diffusion, otherwise, the diffusivities are too low [4]. The device has three important facilities, the first one is the reduction of noise since the introduction of the (n) diffused layer achieves purer hole injection into the avalanche region,the second is the enhancement of the response speed due to the built in field that exists between the (n^+) and (n) layer,and finally, the series resistance that rises due to the effect of an unswept epitaxial layer and this rising reduces the terminal negative resistance of the device [5].

3. Doping Profile

As we see from Fig(1) , N_b is the background concentration which is the concentration in the p-layer, the diffusion coefficient in the (n) layer varies with dopant concentration, i.e. extrinsic diffusion. The diffusion coefficient, D_s , is also called the surface diffusivity for $n > n_i$ can be written as

$$D_s = D_n^{\backslash} e^{-E_a^{\backslash}/KT} \left[\frac{n}{n_i} \right] \quad \dots\dots\dots\dots\dots\dots\dots\dots\dots\dots\dots\dots\dots\dots\dots\dots\dots\dots\dots\dots\dots.(1)$$

Where $D_n^\backslash$ is $45.8 \ cm^2/s$, $E_a^\backslash$ is 4.05 eV, K is the Boltzman's constant, T is the temperature, n_i is the intrinsic-carrier concentration and n is the carrier concentration which equals to the dopant concentration [6]. The junction depth, w_j, is independent of the background p-type concentration and is given by

$$w_j = 1.6 \left[D_n^\backslash \ e^{-E_a^\backslash / KT} \left\{ \frac{N_s}{n_i} \right\} t \right]^{1/2} \ \dots \dots \dots \dots \dots \dots \dots \dots \dots \dots (2)$$

Where N_s is the surface concentration and t is the diffusion time.The representation of the doping profile,N, in the (n) layer is a Chebyshev orthogonal polynomial given by [7]

$$N = N_s \left(1 - 0.87 \frac{x}{\sqrt{4D_s t}} - 0.45 \frac{x^2}{4D_s t} \right) \dots \dots \dots \dots \dots \dots \dots \dots \dots .(3)$$

Where x is the distance from the surface and D_s is given by Eq.1 where $n = N_s$.

4. Electric Field Distribution

The depletion layer thickness, w, that forms at the n-p junction has two components, w_n at the n-side and w_p at the p-side , is treated with the assumption of the complete ionization of donors and acceptors. The Poisson's equation is given by

$$\frac{d^2Q}{dx^2} = \frac{-dE}{dx} = \frac{-\rho}{K_c \varepsilon_O} = \frac{-qN_s}{K_c \varepsilon_O} \left[\left(1 - 0.87 \frac{x}{\sqrt{4D_s t}} - 0.45 \frac{x^2}{4D_s t} \right) - \frac{N_b}{N_s} \right] \dots \dots \dots \dots \dots \dots (4)$$

Where Q is the electrostatic potential, E is the electric field, k_c is the dielectric constant, ρ is the net density of positive charge, ε_o is the permittivity of free space, and q is the electronic charge.

The electric field is obtained by equations obtained from analytical solution of Poisson's equation and the use of MATLAB. The electric field vanishes at depletion layer boundaries. The expression of the field distribution on the two sides of the junction is given by

$$E_1(x) = \frac{qN_s}{k_c \varepsilon_O} \int_{w_j - w_n}^{x} \left[\left(1 - 0.87 \frac{x}{\sqrt{4D_s t}} - 0.45 \frac{x^2}{4D_s t} \right) - \frac{N_b}{N_s} \right] dx \dots \dots \dots \dots \dots \dots .(5)$$

on the left side of the junction, and

$$E_2(x) = \frac{qN_s}{k_c\varepsilon_O} \int_x^{w_j+w_p} \left[\left(1 - 0.87\frac{x}{\sqrt{4D_s t}} - 0.45\frac{x^2}{4D_s t} \right) - \frac{N_b}{N_s} \right] dx \ldots\ldots\ldots\ldots\ldots\ldots\ldots\ldots(6)$$

on the right side of the junction .The integration of Eq.5 gives

$$E_1(x) = \frac{qN_s}{k_c\varepsilon_O} \left\{ x - \frac{0.87}{4\sqrt{D_s t}}x^2 - \frac{0.45}{12D_s t}x^3 - \frac{N_b}{N_s}x \right\} + C_1 \ldots\ldots\ldots\ldots\ldots\ldots\ldots\ldots(7)$$

where C_1 is a constant of integration that can be found from the boundary condition that

$$E_1(x)=0 \quad at \quad x = w_j - w_n \ldots\ldots\ldots\ldots\ldots\ldots\ldots\ldots\ldots\ldots\ldots(8)$$

Thus

$$C_1 = -\frac{qN_s}{k_c\varepsilon_O}\left\{ \left(1-\frac{N_b}{N_s}\right)(w_j - w_n) - \frac{0.87}{4\sqrt{D_s t}}(w_j - w_n)^2 - \frac{0.45}{12D_s t}(w_j - w_n)^3 \right\}\ldots\ldots\ldots\ldots(9)$$

Therefore, the electric field at the left side of the junction is given by

$$E_1(x) = \frac{qN_s}{k_c\varepsilon_O}\left\{ \left(1-\frac{N_b}{N_s}\right)[x - (w_j - w_n)] - \frac{0.87}{4\sqrt{D_s t}}\left[x^2 - (w_j - w_n)^2\right] - \frac{0.45}{12D_s t}\left[x^3 - (w_j - w_n)^3\right] \right\}\ldots\ldots(10)$$

Similarly, the electric field at the right side of the junction is given by

$$E_2(x) = \frac{qN_s}{k_c\varepsilon_O}\left\{ \left(1-\frac{N_b}{N_s}\right)[x - (w_j + w_p)] - \frac{0.87}{4\sqrt{D_s t}}\left[x^2 - (w_j + w_p)^2\right] - \frac{0.45}{12D_s t}\left[x^3 - (w_j - w_n)^3\right] \right\}\ldots\ldots(11)$$

The peak field is found at $x = w_j$, substitute on into Eq.10 and Eq.11 gives

$$E_1(w_j) = \frac{qN_s}{k_c\varepsilon_O}\left\{ w_n\left[1-\frac{N_b}{N_s}\right] - \frac{0.87}{4\sqrt{D_s t}}\left[w_j^2 - (w_j - w_n)^2\right] - \frac{0.45}{12D_s t}\left[w_j^3 - (w_j - w_n)^3\right] \right\}\ldots\ldots(12)$$

and

$$E_2(w_j) = \frac{qN_s}{k_c\varepsilon_O}\left\{ w_p\left[\frac{N_b}{N_s}-1\right] - \frac{0.87}{4\sqrt{D_s t}}\left[w_j^2 - (w_j + w_p)^2\right] - \frac{0.45}{12D_s t}\left[w_j^3 - (w_j + w_p)^3\right] \right\}\ldots\ldots(13)$$

Since the peak field is continuous at the junction and at this point the relation between the depletion region components w_n and w_p can be found using iterative method by the following procedures

i – The continuity of the field at the junction means $E_1 (w_j, N_b / N_s, w_n) = E_2 (w_j, N_b / N_s, w_p)$.

ii - Choosing a specific value of w_j, N_b, N_s, w_n so that w_p can be found numerically.

iii - Newton's method is used for rapid convergence of w_p.

iv - With the aid of -i-, finding function of w_p noting that $E_1 (w_j) = E_2 (w_j)$.

v - The function of w_p is called $F (w_p)$ and is given by

$$F(w_p) = \left(1 - \frac{N_b}{N_s}\right)\left[w_n + w_p\right] + \frac{0.87}{4\sqrt{D_s t}}\left[(w_j - w_n)^2 - (w_j + w_p)^2\right] + \frac{0.45}{12 D_s t}\left[(w_j - w_n)^3 - (w_j + w_p)^3\right]$$

………....……....……....……....……....……....……....……....……....……....……...……(14)

vi - Evaluating $F^{\backslash}(w_p)$.

$$F^{\backslash}(w_p) = \left(1 - \frac{N_b}{N_s}\right) - \frac{0.87}{2\sqrt{D_s t}}\left(w_j + w_p\right) - \frac{0.45}{4 D_s t}\left(w_j + w_p\right)^2 \dots\dots\dots\dots\dots\dots\dots(15)$$

vii- Evaluating of w_p

$$w_p = w_p - \frac{F(w_p)}{F^{\backslash}(w_p)} \dots\dots\dots\dots\dots\dots\dots\dots\dots\dots\dots(16)$$

The algorithm that performs the Newton's method is indicated in Fig(2A) [8]. The plotting of the electric field against the distance is performed in three cases using three different concentration profiles in the n-layer by varying the diffusion time, i.e., the junction depth is varied as shown from Fig(2) before.The electric field distribution is shown in Fig(3) for different junction depths, the value of the maximum field at the junction is decreasing with increasing junction depth and that is because of the decrease in the impurity gradient as shown in Fig(1) before.The width of the depletion layer is increased since it is inversely proportional to the impurity gradient. The value of the maximum field versus the depletion layer width is well demonstrated in Fig(4).

5. Potential Distribution

The integration of Poisson's equation, Eq.4, once again gives the potential distribution. Let us call $V_1(x)$ and $V_2(x)$ the potential distribution at the left side and at the right side of the junction respectively. So

$$V_1(x) = - \int_{w_j - w_n}^{x_j} E_1(x)\ dx \dots\dots\dots\dots\dots\dots\dots\dots\dots\dots\dots\dots\dots(17)$$

$$V_1(x) = -\frac{qN_s}{K_c\varepsilon_O}\left\{\left(1-\frac{N_b}{N_s}\right)\left[\frac{1}{2}x^2 - x\left(w_j - w_n\right)\right] - \frac{0.87}{4\sqrt{D_s t}}\left[\frac{1}{3}x^3 - x\left(w_j - w_n\right)^2\right] - \frac{0.45}{12D_s t}\left[\frac{1}{4}x^4\right.\right.$$

$$\left.\left. - x\left(w_j - w_n\right)^3\right]\right\} + C_2 \dots\dots\dots\dots\dots\dots\dots\dots\dots\dots\dots\dots\dots\dots\dots(18)$$

With the boundary condition

$$V_1(x) = 0 \qquad at \qquad x = w_j - w_n \dots\dots\dots\dots\dots\dots\dots\dots\dots\dots\dots\dots\dots\dots\dots(19)$$

$$C_2 = \frac{qN_s}{k_c\varepsilon_O}\left\{\left(1-\frac{N_b}{N_s}\right)\left[-\frac{1}{2}\left(w_j - w_n\right)^2\right] - \frac{0.87}{4\sqrt{D_s t}}\left[-\frac{2}{3}\left(w_j - w_n\right)^3\right] - \frac{0.45}{12D_s t}\left[-\frac{3}{4}\left(w_j - w_n\right)^4\right]\right\} \dots(20)$$

$$V_1(x) = -\frac{qN_s}{k_c\varepsilon_O}\left\{\left(1-\frac{N_b}{N_s}\right)\left[\frac{1}{2}x^2 - x\left(w_j - w_n\right) + \frac{1}{2}\left(w_j - w_n\right)^2\right] - \frac{0.87}{4\sqrt{D_s t}}\left[\frac{1}{3}x^3 - x\left(w_j - w_n\right)^2 + \frac{2}{3}\left(w_j - w_n\right)^3\right] - \right.$$

$$\left.\frac{0.45}{12D_s t}\left[\frac{1}{4}x^4 - x\left(w_j - w_n\right)^3 + \frac{3}{4}\left(w_j - w_n\right)^4\right]\right\} \dots\dots\dots\dots\dots\dots\dots\dots\dots\dots\dots(21)$$

Similarly

$$V_2(x) = -\int_x^{w_j+w_p} E_2(x)\,dx \dots\dots\dots\dots\dots\dots\dots\dots\dots\dots\dots\dots\dots\dots\dots\dots\dots(22)$$

With the boundary condition

$$V_2(x) = V_1(w_j) \qquad at \qquad x = w_j \dots\dots\dots\dots\dots\dots\dots\dots\dots\dots\dots\dots\dots\dots(23)$$

Let C_3 be the constant of integration in Eq.22, so C_3 is given by

$$C_3 = -\frac{qN_s}{K_c\varepsilon_O}\left\{\left(1-\frac{N_b}{N_s}\right)\left[w_j\left(w_n + w_p\right) + \frac{1}{2}\left(w_j - w_n\right)^2\right] + \frac{0.87}{4D_s t}\left[w_j\left[\left(w_j - w_n\right)^2 - \left(w_j + w_p\right)^2\right] - \frac{2}{3}\right.\right.$$

$$\left.\left.\left(w_j - w_n\right)^3\right] + \frac{0.45}{12D_s t}\left[w_j\left[\left(w_j - w_n\right)^3 - \left(w_j + w_p\right)^3\right] - \frac{3}{4}\left(w_j - w_n\right)^4\right]\right\} \dots\dots\dots\dots(24)$$

So $V_2(x)$ can be written as

$$V_2(x) = -\frac{qN_s}{K_c\varepsilon_O}\left\{\left(1-\frac{N_b}{N_s}\right)\left[\frac{1}{2}x^2 - x\left(w_j + w_p\right) + w_j\left(w_n + w_p\right) + \frac{1}{2}\left(w_j - w_n\right)^2\right] - \frac{0.87}{4\sqrt{D_s t}}\left[\frac{1}{3}x^3 - \right.\right.$$

$$\left.x\left(w_j + w_p\right)^2 - w_j\left[\left(w_j - w_n\right)^2 - \left(w_j + w_p\right)^2\right] + \frac{2}{3}\left(w_j - w_n\right)^3\right] - \frac{0.45}{12D_s t}\left[\frac{1}{4}x^4\right.$$

$$\left.\left. - x\left(w_j + w_p\right)^3 - w_j\left[\left(w_j - w_n\right)^3 - \left(w_j + w_p\right)^3\right] + \frac{3}{4}\left(w_j - w_n\right)^4\right]\right\} \dots\dots\dots\dots\dots\dots(25)$$

The potential distribution for different junction depths is shown in Fig(5). From the observation of this figure, it can be seen that the potential is increased with increasing junction depth because the depletion layer is widened and it is proportional to the built- in field.

6. Avalanche Multiplication & Noise considerations

Impact ionization means the releasing of new electron-hole pairs from carriers that drift at a saturation velocity when high-electric field is applied .Impact ionization may occur when a carrier has enough energy to initiate a transition of an electron from a valence band into a conduction band. The smallest energy required for such a process, consistent with energy and momentum conservation, is called the threshold energy [9].The impact ionization is characterized by the ionization rates (α_n) and (α_p) for electrons and holes . The impact ionization coefficients of electrons and holes for silicon are given by [10]

$$\alpha_n = 3.8*10^6 e^{-\frac{1.75*10^6}{E}} \quad\ldots\ldots\ldots\ldots\ldots\ldots\ldots\ldots\ldots\ldots\ldots\ldots\ldots\ldots\ldots\ldots\ldots\ldots\ldots\ldots\ldots\ldots(26)$$

$$\alpha_p = 2.25*10^7 e^{-\frac{3.26*10^6}{E}} \quad\ldots\ldots\ldots\ldots\ldots\ldots\ldots\ldots\ldots\ldots\ldots\ldots\ldots\ldots\ldots\ldots\ldots\ldots\ldots(27)$$

where *E* is the electric field. In our device model, the electrons will be swept by the electric field to the left and holes to the right. An approximate analysis for the avalanche multiplication of carriers is used. Let the carriers (holes) be accelerated through a depletion region (*w*) that has a probability p of creating an electron-hole pair by undergoing ionizing collision. Then for p$_{in}$ incoming holes entering the depletion region from the n-region, Pp$_{in}$ is the secondary electron hole pair that it will be generated and so on. Assuming no recombination, the total number of holes coming out of the depletion region in the p-region is obtained as[11],

$$p_{out} = p_{in}(1 + P + P^2 + P^3 + {}^{\cdots\cdots}) \ldots\ldots\ldots\ldots\ldots\ldots\ldots\ldots\ldots\ldots\ldots\ldots\ldots\ldots\ldots\ldots(28)$$

Therefore, the multiplication factor of holes is given by

$$M_h = \frac{p_{out}}{p_{in}} = (1 + P + P^2 + P^3 + \ldots\ldots) = \frac{1}{1-P} \ldots\ldots\ldots\ldots\ldots\ldots\ldots\ldots\ldots\ldots\ldots\ldots(29)$$

The probability of an ionizing collision as a carrier travels through the depletion region can also be expressed as [12]

$$\int_0^w \alpha_p \exp\left[-\int_0^x (\alpha_p - \alpha_n)dx^{\backslash}\right]dx = 1 \ldots\ldots\ldots\ldots\ldots\ldots\ldots\ldots\ldots\ldots\ldots\ldots\ldots\ldots(30)$$

The maximum electric field at breakdown can be calculated from the field dependence of the ionization rates and the breakdown condition .

Noise consideration in the device is due to spontaneous fluctuations in the current passing through or the instability of voltage across the semiconductor device. The multiplication noise will set lower limit to the signal to be amplified. However; new technologies can reduce this noise [13].

The multiplication process buildup is aided by the hole feedback mechanism. The feedback greatly depends on the impact ionization coefficient ratio between electrons and holes and is more pronounced as

the symmetry in the carrier ionization coefficient becomes larger. The ratio of the hole to electron ionization coefficients (K_p) is given by

$$K_p = \frac{\alpha_p}{\alpha_n} \dots\dots\dots\dots\dots\dots\dots\dots\dots\dots\dots\dots\dots\dots\dots\dots (31)$$

And the excess noise factor , ENF, is given by [14] .

$$ENF = M_h \left[1 + \left(\frac{1 - K_p}{K_p} \right) \left(\frac{M_h - 1}{M_h} \right)^2 \right] \dots\dots\dots\dots\dots\dots\dots\dots\dots\dots\dots (32)$$

Where M_h is the multiplication factor for injected holes.

The excess noise, a function of multiplication factor, is shown in Fig(6), and is decreased with increasing the junction depth since this leads to higher hole to electron ionization rate ratio.

7. Response Speed

The length of the depletion region plays an important role in the evaluation of the transit time which depends greatly on that length. The diffusion time in the undepleted layer is the second factor that determines the response speed and this time depends on the width of the depletion region in the n-layer (w_n). The third factor is the time required for the avalanche to develop and is called the avalanche build up time which depends greatly on the ratio of the hole to electron impact-ionization coefficients and this time decreases as this ratio becomes small. The three time constants that determine the response speed of the IMPATT diode are given by

$$t_s = \frac{2\left(w_n + w_p\right)}{v_s} + \frac{\left(w_j - w_n\right)^2}{2.4 D_p} + \left(\frac{\alpha_p}{\alpha_n} \right) \left(\frac{X_A}{v_s} \right) M \dots\dots\dots\dots\dots\dots\dots (33)$$

Where t_s is the overall transit time, v_s is the saturation velocity, D_p is the diffusivity of holes, M is the multiplication factor and X_A is the length of the avalanche region.

It can be seen from the Eq.33 that the third term which represents the avalanche build-up time is small that it can be neglected during the analysis, so the first two terms determine the response speed of the IMPATT diode. The time needed for the holes to cross the depletion region is increased with increasing the depletion layer width as shown in Fig(7), and the time in the undepleted region is increased with increasing the junction depth in spite of the increasing of the length of the component of the depletion layer in the left side of the junction (w_n), and this is depicted in Fig(8).

8. Output Power

The maximum output power is limited by the semiconductor device material and the impedance level in the microwave circuitry. At a given frequency the limitation of semiconductor material is the electrical field at breakdown and the saturation velocity. The power output, P_m , which is the most important figure of merit of the IMPATT microwave device is given by

$$P_m = \frac{0.5 \, K_c \, \varepsilon_O \, A \, E_c^2 \, v_s^2}{(w_n + w_p) f} \dots\dots\dots\dots\dots\dots\dots\dots\dots\dots\dots\dots\dots\dots\dots\dots\dots\dots\dots\dots (34)$$

Where f is the frequency, A is the device area, and E_c is the critical field at breakdown. The IMPATT diode has high operating field at avalanche breakdown so the device has high $P_m f^2$ product.

The output power as a function of frequency is depicted in Fig(9), the power is decreased with increasing the frequency. Also it can be seen that the output power is decreased with increasing the depletion layer width. The overall modeling process employed in the analysis is depicted in Fig(10).

9. Conclusion

The results obtained from the computer aided analysis of n^+- n - p – p^+ silicon IMPATT diode state that the junction depth in the n - p layer is independent of the background p-type concentration, and when the concentration near the n - p junction is sharper in decreasing , i.e. the gradient is in its lower value, the value of the maximum field at the junction is in its lowest value. So to increase the value of the maximum field when the device is operated at breakdown condition, the junction depth should be increased and this increase also increases the built in potential that exists at the boundaries of the depletion layer width.

The depletion layer dependence of response speed of the device affects both the time needed for the carriers to cross the depletion region and the time needed for the carriers in the undepleted layer, however, the first one which is the more important is increased. The continuous wave output power becomes less in higher depletion region width.

The excess noise factor, which is one of the most important parameters that should be taken into consideration, is smaller in deeper junctions because of the higher electric field due to wider depletion region width. So in the design of the device for a certain application; tradeoff should be made between the forementioned parameters.

ALGORITHM NEWTON (F, $F^{\textasciigrave}$, W_p, E, N_i)

This algorithm computes a solution of $F(w_p) = 0$ given an initial approximation x_o (starting value of the iteration). Here the function F is continuous and has continuous derivative $F^{\textasciigrave}$.

INPUT: F, $F^{\textasciigrave}$, initial approximation x_o, tolerance $\epsilon > 0$, maximum number of iterations N_i.

OUTPUT: Approximate solution w_p ($p \leq Ni$) of message of failure.
For   p = 0, 1, 2,…………, N-1 do :

1   Compute $F^{\textasciigrave}(w_p)$
2   If $F^{\textasciigrave}(w_p) = 0$ then OUTPUT "Failure". stop.
    [Procedure completed unsuccessfully].
3   Else compute

$$w_{p+1} = w_p - \frac{F(w_p)}{F^{\textbackslash}(w_p)}$$

4   If $| w_{p+1} - w_p | \leq \epsilon | w_p|$ then OUTPUT w_{p+1} stop .
    [Procedure completed unsuccessfully].

   END

5   OUTPUT "Failure". Stop.
        [Procedure completed unsuccessfully after N_i iterations].

   END NEWTON

Fig.(A) An algorithm for evaluation of the depletion region component in the p-side using Newton's method.
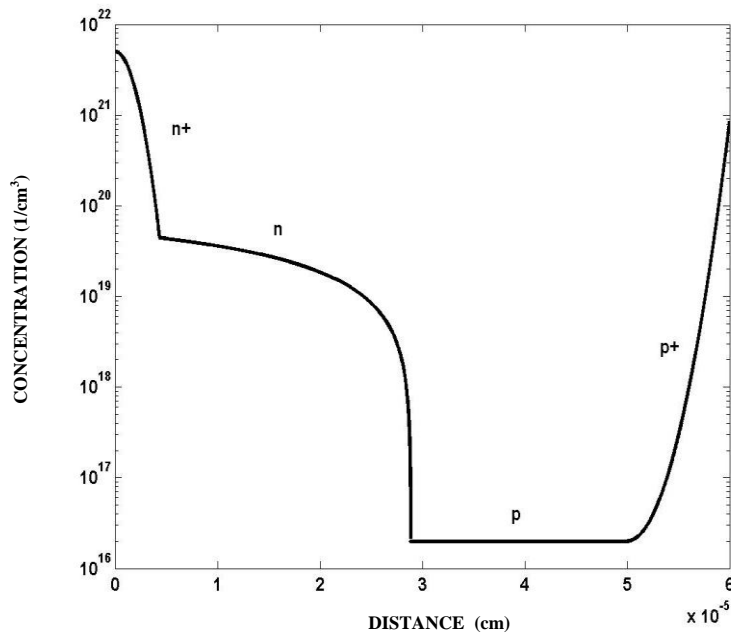
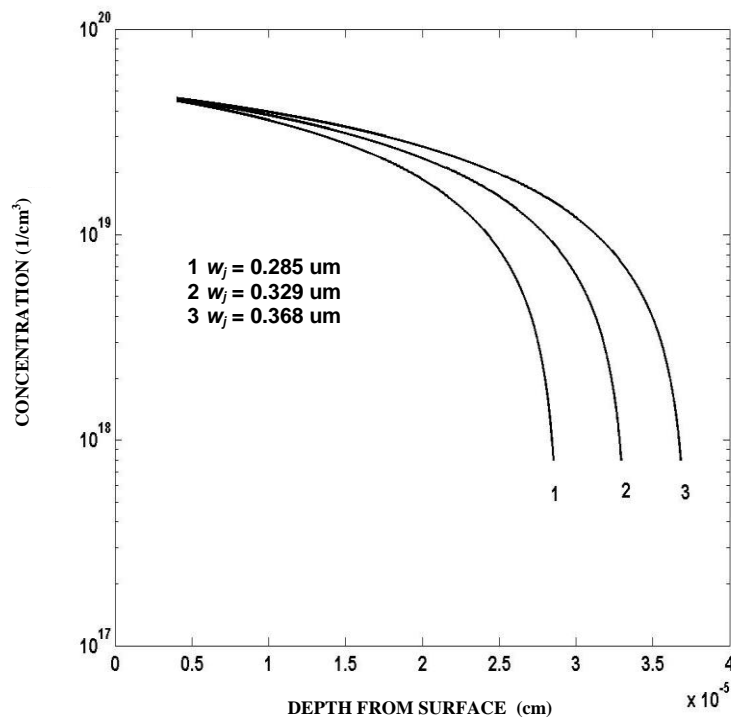**Fig.(1) Doping profile of n+-n-p-p+ silicon IMPATT diode.**

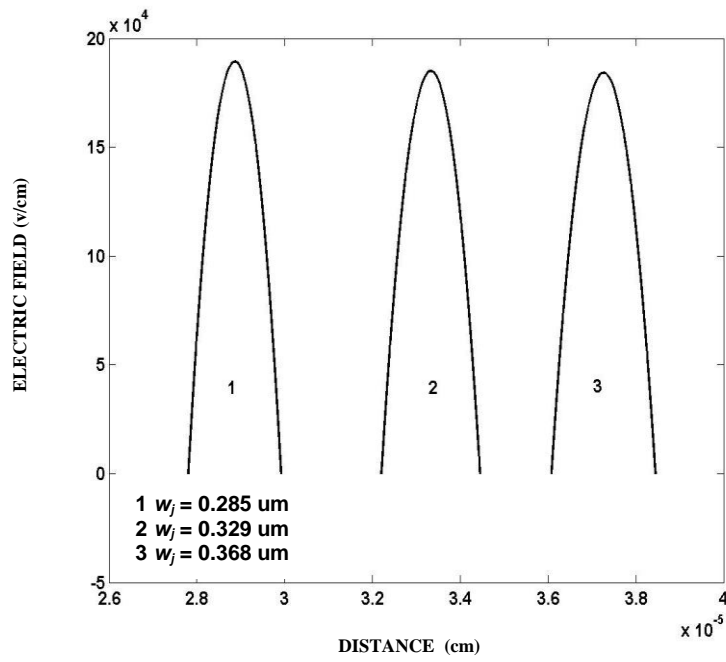**Fig.(2) Doping profiles in the (n) layer for different junction depths.**

١١

Fig.(3) Calculated electric field distributions.
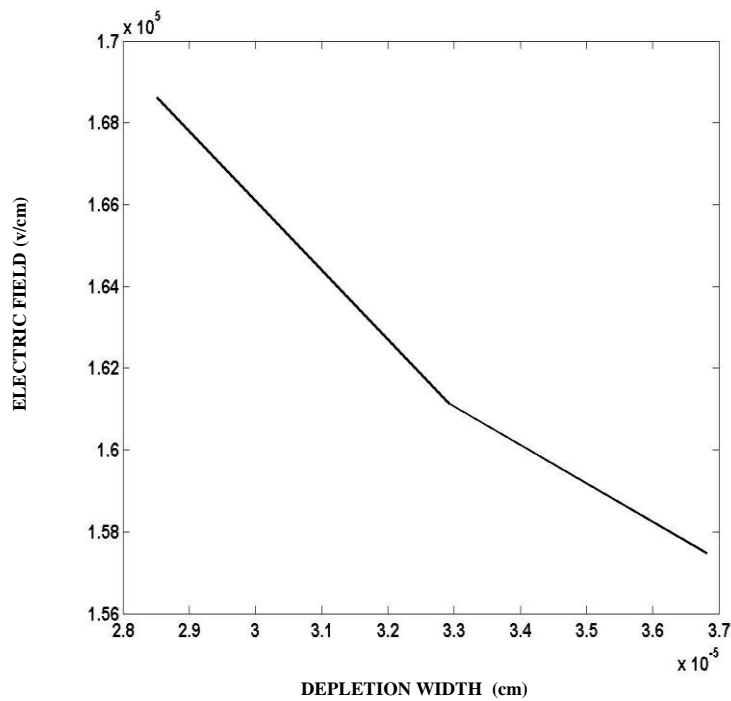

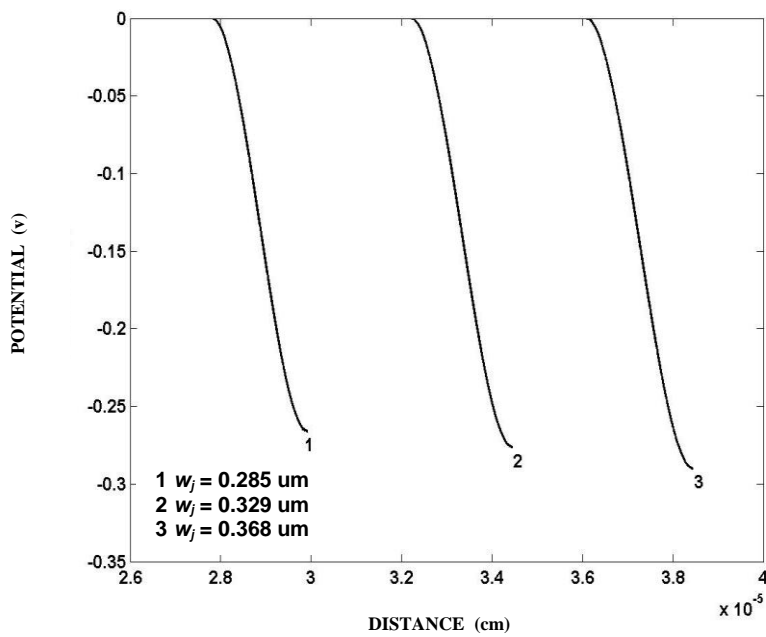**Fig.(4) Electric field versus depletion width.**
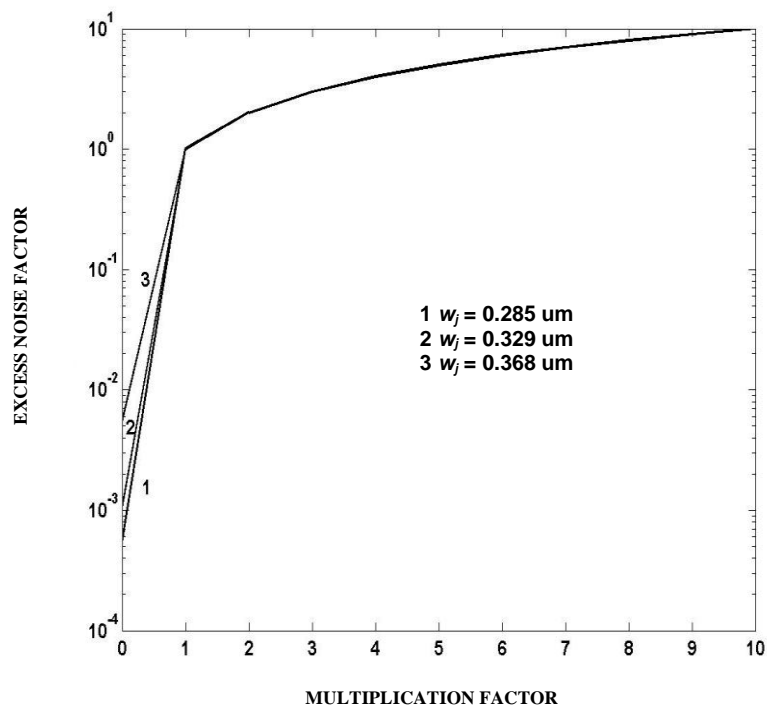
Fig.(5) Calculated potential distributions.

Fig.(6) Calculated excess noise factor as a function of multiplication factor for different junction depths.
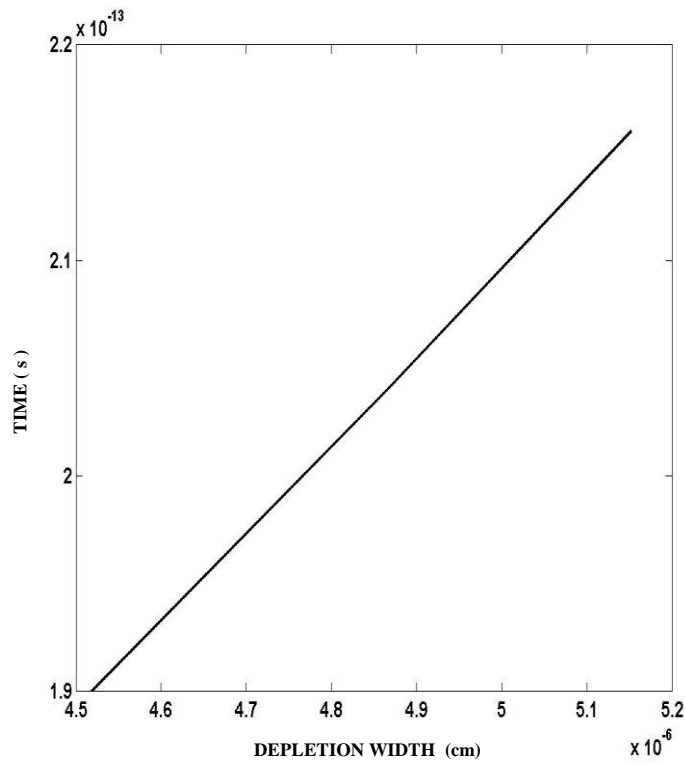
Fig.(7) Time needed for holes to cross the depletion region as a function of depletion width.
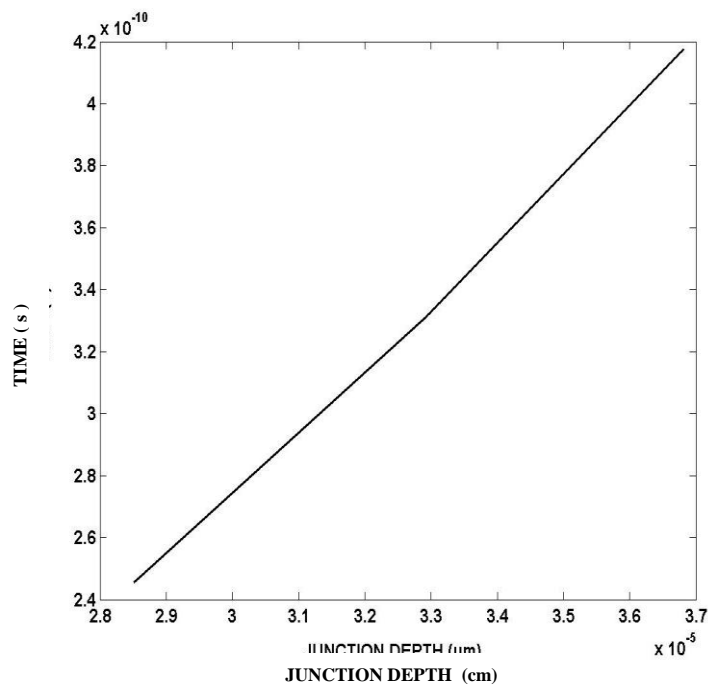

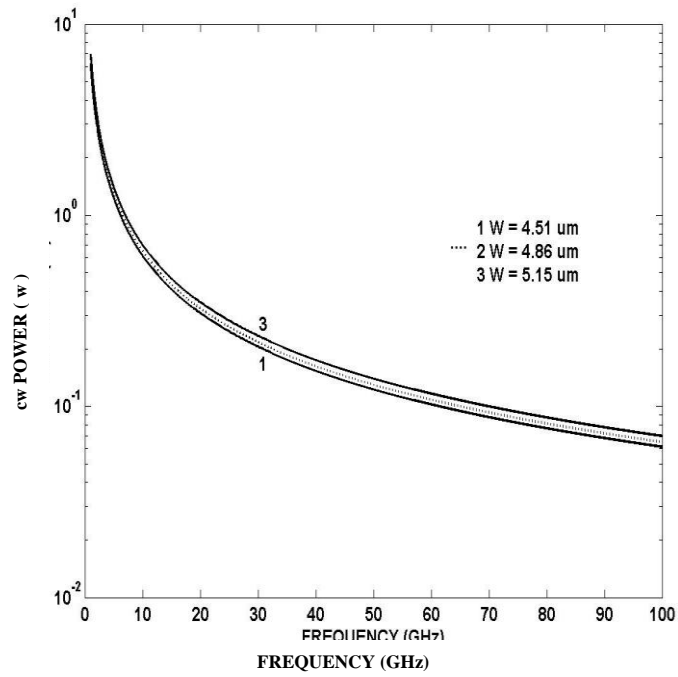**Fig.(8) Time in the undepleted region as a function of junction depth.**

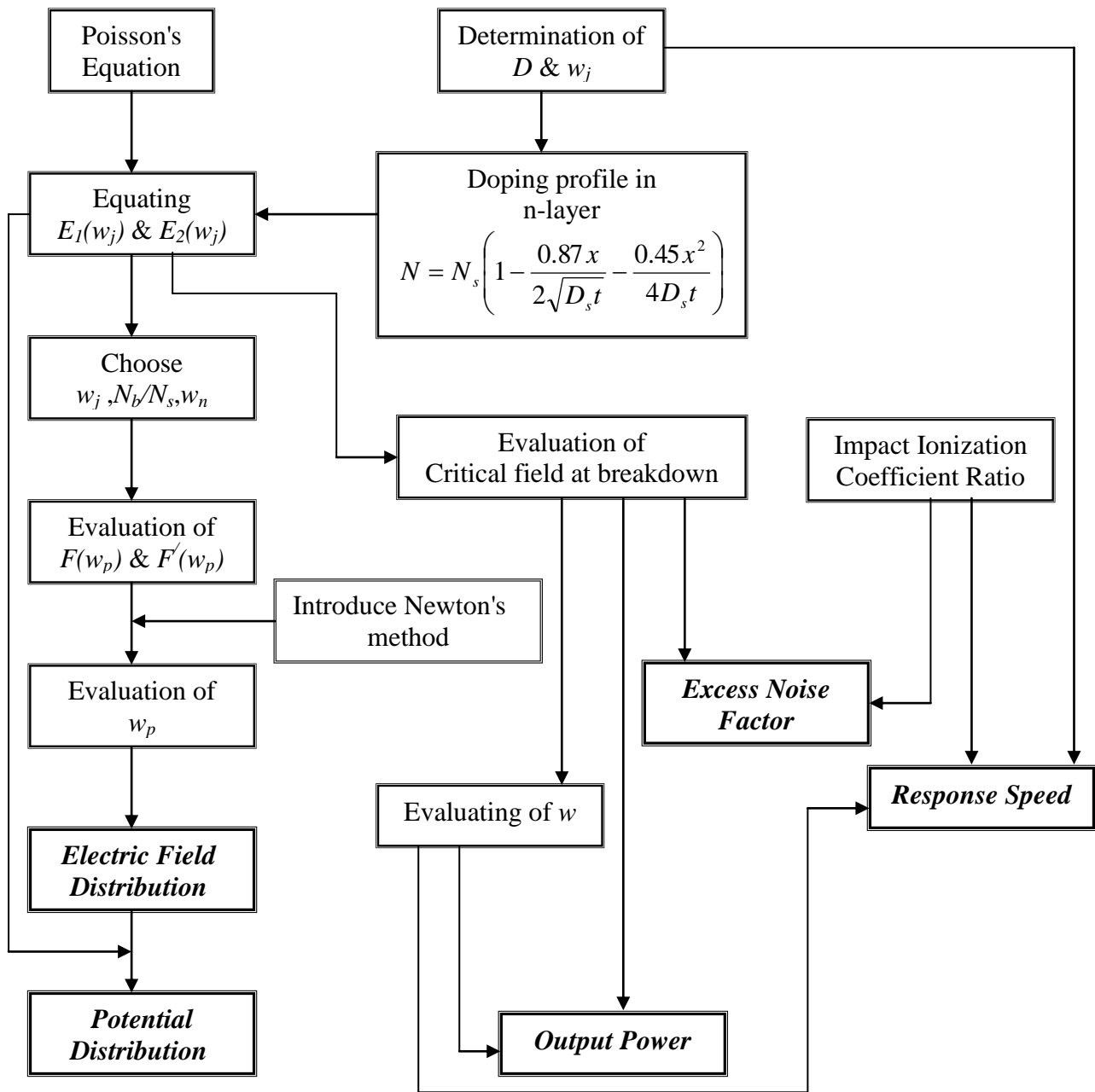**Fig.(9) Power output versus frequency for different depletion layer width.**

Poisson's Equation

Determination of D & w_j

Equating $E_1(w_j)$ & $E_2(w_j)$

Doping profile in n-layer

$$N = N_s\left(1 - \frac{0.87\,x}{2\sqrt{D_s t}} - \frac{0.45\,x^2}{4D_s t}\right)$$

Choose w_j, N_b/N_s, w_n

Evaluation of Critical field at breakdown

Impact Ionization Coefficient Ratio

Evaluation of $F(w_p)$ & $F'(w_p)$

Introduce Newton's method

Evaluation of w_p

Excess Noise Factor

Electric Field Distribution

Evaluating of w

Response Speed

Potential Distribution

Output Power

Fig.(10) Block diagram of the modeling process for a static characteristics
        of an n+-n-p-p+ silicon IMPATT diode.

10. References

1. Y. Aono and Y. Okuto,*" Effect of Undepleted High Resistivity Region on Microwave Efficiency of GaAs IMPATT Diodes, "* proc.IEEE, vol.63, PP.724, 1975.

2. R.B.Fair *," Concentration Profiles of Diffused Dopants, "* in F.F.Y.wang ,Ed.,Impurity Doping processes in Silicon, North-Holland , Amsterdam,1981.

3. S.M.Sze , *" VLSI Technology, "* McGraw-Hill,1988.

4. Erwin Kreszig *,"Advanced Engineering Mathematics,"* John Wiley & Sons , INC ,1999.

5. Michael Shur, *"Physics of Semiconductor Devices,"* Prentice-Hall of India, 1995.

6. S.M.Sze and G.Gibbons,*" Avalanche Breakdown voltages of Abrupt and Linearly Graded P-N Junction in Ge ,Si ,GaAs , and GAP, "* Bell Telephon Laboratories , Jan .1966.

7. Nadita Das Gupta and Amitava Das Gupta,*"Semicoductor Devices : Modelling and Technology, "* Prentice-Hall of India, 2004.

8. S.M.Sze,*" Physics of Semiconductor Device, "* 2nd.ed., wiley, 1981.

9. M.A.Al.Kaiat,*" Avalanche Photodiode Modelling,"* M.Sc Thesis, University of Technology, Baghdad –Iraq, Sep.1989.

10. R.J.Mc Intyre,*" Multiplication Noise in Uniform Avalanche Diodes,"* IEEE Trans.Electron Devices, vol.ED-13, PP.164-168, Jan.1966.

11. W.E. Schroeder and G.I. Haddad,*" Nonlinear Properties of IMPATT Devices, "* Proc.IEEE, vol.61, PP 153, 1973.

12. Special Issue on *solid-state Microwave Millimeter - wave power Generation, Amplification, and Control*, IEEE Trans. Microwave Theory Tech.MTT-27, May.1979.

13. S.M. Sze *," Semiconductor Devices , Physics and Technology, "* John Wiley & sons,1985 .

14. B.G.Streetman and S.Banerjee, *"Solid State Electronic Devices,"* Prentice Hall, 2000